THE BELL SYSTEM TECHNICAL JOURNAL
Vol. 52, No. 10, December, 1973
Printed in U.S.A.

Phase Dispersion Characteristics During Fade in a Microwave Line-of-Sight Radio Channel

By M. SUBRAMANIAN, K. C. O'BRIEN, and P. J. PUGLIS

(Manuscript received February 5, 1973)

Measurements of phase and amplitude dispersion over a 20-MHz band have been made on a 42-km, 6-GHz, line-of-sight microwave link. A novel technique is introduced for measuring the phase dispersion induced by the propagation path. Specifically, the amplitudes and relative phases of four tones separated equally by 6.6 MHz have been continuously monitored over a period of four months. The data show that there is usually measurable (0.02 degree/(MHz)²) phase distortion over the 20-MHz band during those fades whose depth exceeds about 20 dB. These dispersive fades, which usually last a few seconds, typically occur along with shallow and essentially nondispersive fades that have durations of several minutes. However, only the dispersive fades exhibit a phase nonlinearity. Analysis of 16 events measured in the autumn of 1970 yield the following results.

(*i*) *The distribution curve describing the fraction of time that phase nonlinearity (quadratic) exceeds a given value follows a log-normal distribution.*

(*ii*) *The quadratic phase nonlinear coefficient exceeds an average value of 0.1 degree/(MHz)² for fades with depth larger than 34 dB from the nominal level. This corresponds to a time delay distortion of 0.55 nanosecond over 1-MHz band.*

(*iii*) *The correlation between log-amplitude and phase nonlinear coefficients yields a correlation coefficient whose magnitude is fade-depth dependent and whose sign varies from event to event.*

The experimental technique of measuring phase dispersion reported here may be of interest not only for propagation studies but also in other systems such as measurement of characteristics of electrical networks. The statistical results obtained on the phase characteristics may prove of interest in formulating an analytical model. Further, they may be of significance in the design of existing and future microwave systems.

I. INTRODUCTION

Fading in microwave communication channels has been the subject of investigation by many workers for a considerable length of time. However, the emphasis on these studies has been more toward the behavior of the amplitude characteristics of the signal rather than of its phase characteristics. The purpose of this study was to investigate the phase characteristics of a microwave signal transmitted over a typical tropospheric, line-of-sight link.* Specifically, the following topics were addressed in the experiment.

(*i*) Measurement of phase variations over a microwave radio channel, as a function of both frequency and time; obtaining from the experimental results statistics on the phase nonlinearity in a microwave radio channel.

(*ii*) Correlation, if any, between the amplitude and phase distortions.

Measurements were made in late 1970 on a TH-3 radio channel operating between Atlanta and Palmetto, Georgia. The experiment was conducted as an adjunct to an ongoing study by other members of Bell Laboratories. The transmitter located in Atlanta and the front end of the receiver situated in Palmetto were common to both experiments. However, a different set of apparatus was employed for the measurement of amplitude and phase in the present study. G. M. Babler[1] has reported on the experimental layout of the microwave link.

This paper addresses three major areas: experimental technique and arrangement, measured data, and statistical analysis. The experimental technique is a novel one in that it measures directly the phase difference between pairs of transmitted tones separated in frequency. Only the phase difference induced by the propagation path is measured, not the transmitter and receiver beat oscillator fluctuations. More specifically, at a carrier frequency of 6 GHz, four tones separated by 6.6 MHz and with a definite phase relation are transmitted over a 42-km line-of-sight path. At the receiving end, the signals are brought to a 70-MHz IF and filtered out. The amplitude of each tone is continuously monitored. The phase difference between each adjacent pair is measured.

Data were recorded during roughly 100 events in which the fade

* As a result of the findings reported here, a more comprehensive, higher resolution measurement program has been undertaken to characterize more completely the dispersive microwave channel. It is expected that a summary of these results will be published here in the near future.

depth exceeded 10 dB. These fades can generally be divided into two categories. The majority of them are relatively shallow (<20 dB), long-lasting (minutes) events which show little amplitude and nonlinear phase distortion, although linear phase dispersion corresponding to path length variations may be observed. A second class of events are those that exhibit deep and brief (seconds) fades showing substantial amplitude dispersion and nonlinear phase dispersion. This second class could present difficulties to communication systems.

Twenty-six dispersive fading events whose fade depth exceeded 20 dB were observed during the autumn of 1970, a smaller number than usual. Only 16 of these were analyzable as a result of equipment malfunction. This analysis yielded the following results.

(*i*) The distribution curve describing the fraction of time that the phase nonlinearity (quadratic) exceeds a given value follows an almost log-normal distribution.

(*ii*) The quadratic phase nonlinear coefficient exceeds an average value of 0.1 degree/(MHz)^2 for fades that are deeper than 34 dB from the nominal level. This corresponds to a time delay distortion of 0.55 nanosecond over 1-MHz band.

(*iii*) No simple relationship seems to exist for the correlation between the quadratic log-amplitude and the quadratic phase nonlinear coefficients.

II. DESCRIPTION OF PHASE DISPERSION MEASUREMENT

This experiment measures the effect of the transmission path on the relative phase of signals at different frequencies. Specifically, a "picket fence" of tones in the 6-GHz range, separated from each other by 0.55 MHz, are transmitted over an approximately 42-km path. These tones are generated at the transmitter by means of a "picket-fence" generator developed by G. A. Zimmerman of Bell Laboratories. The experimental apparatus measures the phase difference between pairs of these tones separated by 6.6 MHz in such a way that only the phase difference induced by the transmission path is measured, and not the transmitter and receiver beat oscillator fluctuations. Although a closer spacing between the tones would have been more desirable, practical considerations limited the selection to four tones distributed uniformly over the 20-MHz radio channel. Further, at the time of initiation of this experiment, the available statistics[2] on the amplitude dispersion during deep microwave fading did not seem to indicate any significant fine structure over a 20-MHz band, and consequently no fine structure

of phase nonlinearity of significant magnitude was expected as a result of fading by multiray phenomena.

To understand the measurement, it is important to trace a signal all the way through the system. A 70.4-MHz signal inserted into the picket-fence generator is divided by 128 and fed into a pulse generator. The resulting pulses are then mixed with the 70.4-MHz signal producing a picket fence of tones separated by 0.55 MHz and centered at 70.4 MHz. In addition to having equal amplitude, the tones have the same initial phase. The time-dependent frequency error of the 70.4-MHz signal caused by oscillator fluctuations may conveniently be expressed as $128\ \Delta\omega_o\ (t)$. The nth tone can then be written, with $\omega_o = 70.4/128$ MHz, as

$$A_o \cos\left[n(\omega_o + \Delta\omega_o)t\right], \tag{1}$$

where A_o is the amplitude of each picket. Up conversion at the transmitter by a beat oscillator with angular frequency ω_T yields

$$A_T \cos\left(\{[\omega_T + n(\omega_o + \Delta\omega_o)]\}t + \phi_T\right), \tag{2}$$

where A_T is the amplitude of the transmitted up-converted signal and Φ_T is the phase shift introduced by the beat oscillator. After transmission through the atmosphere, the signal becomes

$$A'_T A_n \cos\left\{[\omega_T + n(\omega_o + \Delta\omega_o)]t + \phi_T + \phi_n^a\right\}, \tag{3}$$

where A_n and Φ_n^a are the amplitude and phase modulation introduced by the atmosphere on the nth tone and A'_T is the amplitude of the received signal without any modulation by the atmosphere. Down conversion at the receiver yields

$$A_R A'_T A_n \cos\left\{[\omega_T - \omega_R + n(\omega_o + \Delta\omega_o)]t + \phi_T - \phi_R + \phi_n^a\right\}, \tag{4}$$

where $A_R A'_T A_n$ is now the amplitude of the IF signal, ω_R is the angular frequency of the receiver beat oscillator, and Φ_R is the phase shift introduced by the receiver beat oscillator. Consider that this IF signal is mixed with a signal from a standard oscillator (phase changes are included in $\Delta\omega_s$) described by

$$A_s \cos\left(\omega_s + \Delta\omega_s\right)t. \tag{5}$$

We then have, for the upper and lower sideband signals (ignoring a constant),

$$S_n = A_s A_R A'_T A_n \cos\left\{[\omega_T - \omega_R + n(\omega_o + \Delta\omega_o) \pm (\omega_s + \Delta\omega_s)]t + \phi_T - \phi_R + \phi_n^a\right\}. \tag{6}$$

In order to compare two tones (m and n) with phases Φ_n^a and Φ_m^a, $n > m$, choose

$$\omega_s = \left(\frac{n-m}{2}\right)\omega_o. \tag{7}$$

By appropriate filtering, S_n and S_m are isolated. After being mixed with ω_s, the lower sideband of S_n denoted by S_{nl} and the upper sideband of S_m denoted by S_{mu} are separated, yielding

$$S_{nl} = A_s A_R A_T' A_n \cos\left\{\left[\omega_T - \omega_R + \left(\frac{n+m}{2}\right)\omega_o + n\Delta\omega_o - \Delta\omega_s\right]t + \phi_T - \phi_R + \phi_n^a\right\} \tag{8}$$

$$S_{mu} = A_s A_R A_T' A_m \cos\left\{\left[\omega_T - \omega_R + \left(\frac{n+m}{2}\right)\omega_o + m\Delta\omega_o + \Delta\omega_s\right]t + \phi_T - \phi_R + \phi_m^a\right\}. \tag{9}$$

Measurement of the difference in phase of S_{nl} and S_{mu} yields

$$[(n-m)\Delta\omega_o - 2\Delta\omega_s]t + \phi_n^a - \phi_m^a \equiv \Delta\phi. \tag{10}$$

If the first term is small, we have a direct measure of the quantity of interest. In this case, ω_s and ω_o are derived from similar highly stable sources (Hewlett-Packard 105B quartz oscillators and General Radio 1165 and 1163 frequency synthesizers). The phase drifts, $12\Delta\omega_o t$ and $2\Delta\omega_s t$ [in eq. (10) corresponding to the selected value for $(n-m) = 12$ in the experiment], are approximately -1 degree/day. Note that, if the frequency deviation is the same for both oscillators, even this small phase drift cancels out. Further, the transmitter and receiver oscillators are manually synchronized every day, except on Sundays. However, this small drift produces a running phase difference (which is linear with time) between tones and can be subtracted out during the data analysis by measuring the linear slope before and after a fading event, thus causing no error to the data. The short-term rms frequency deviations (<1 s) are on the order of 1×10^{-8}/ms or 1×10^{-11}/s. At the frequency of 6.6 MHz, this corresponds to a rms phase noise of 0.024 degree. When the picket-fence generator was run directly into the phase and amplitude measurement system, the observed rms phase noise out of the network analyzers was 0.03 degree. This is considerably smaller than the accuracy of the measuring equipment which is ± 1 degree.

Figure 1 is a block diagram of a simplified system. Of the entire assembly of pickets, those numbered "1" and "13" are separated out by the narrow bandpass filters. Both ω_1 and ω_{13} are mixed with an $\omega_s = (\omega_{13} - \omega_1)/2$ derived from the same source. The second pair of filters labeled $[(\omega_1 + \omega_{13})/2]$ separates the appropriate sidebands.

Figure 2 is a block diagram of the actual measuring system. The entire picket fence is received and divided into four channels. In each channel one tone is filtered through. The four frequencies used are 53.35, 59.95, 66.55, and 73.15 MHz, spanning the desired range of approximately 20 MHz, the width of radio channel. The nominal level of the individual tones at the input to the system is approximately −46 dBm.

Each filtered tone is amplified and mixed with a signal of frequency ω_s from the standard oscillator. The output is then split into its two sidebands, thus producing three pairs of signals, each pair having the same frequency difference.

The network analyzer (Hewlett-Packard Model 676A-H05, which is a modified version of 676A to meet our requirements) measures the relative phase (10 mV/degree), the amplitudes (50 mV/dB), and the ratio of the amplitudes of the two input signals. Amplitudes can be measured over a maximum of 80-dB range with up to 0.01-dB resolution and ±1.5-dB accuracy. Phase difference can be measured with up to 0.02-degree resolution and ±1-degree accuracy if the tone levels are not too widely different. The measured results on the system indicate that for tones whose amplitude difference is less than 30 dB, which is well within the limits on requirements of our experiment, these specifications were satisfactorily met. The network analyzer performs its amplitude and phase measuring functions at an IF frequency of 100 kHz. The accuracies quoted above can be achieved only if this 100 kHz is stable to less than 100 Hz. Because of drifts in the beat frequency oscillators at transmitter and receiver, the frequencies of the signals at the input of the network analyzers drift (together) by a few hundred hertz. In order to maintain the network analyzer's IF frequency constant, it is necessary to track these drifts. This is accomplished by sampling in each network analyzer one of the input signals, amplifying it to a constant level, mixing it with a 100-kHz signal, filtering out one (the upper) sideband, and employing this signal as a local oscillator in the network analyzer. The IF strip in the network analyzer then operates at a constant 100 kHz. This arrangement is shown in Fig. 3. The dc voltage outputs of the network analyzers are recorded on a 7-channel FM tape recorder with a dc-to-625-Hz bandwidth. The four

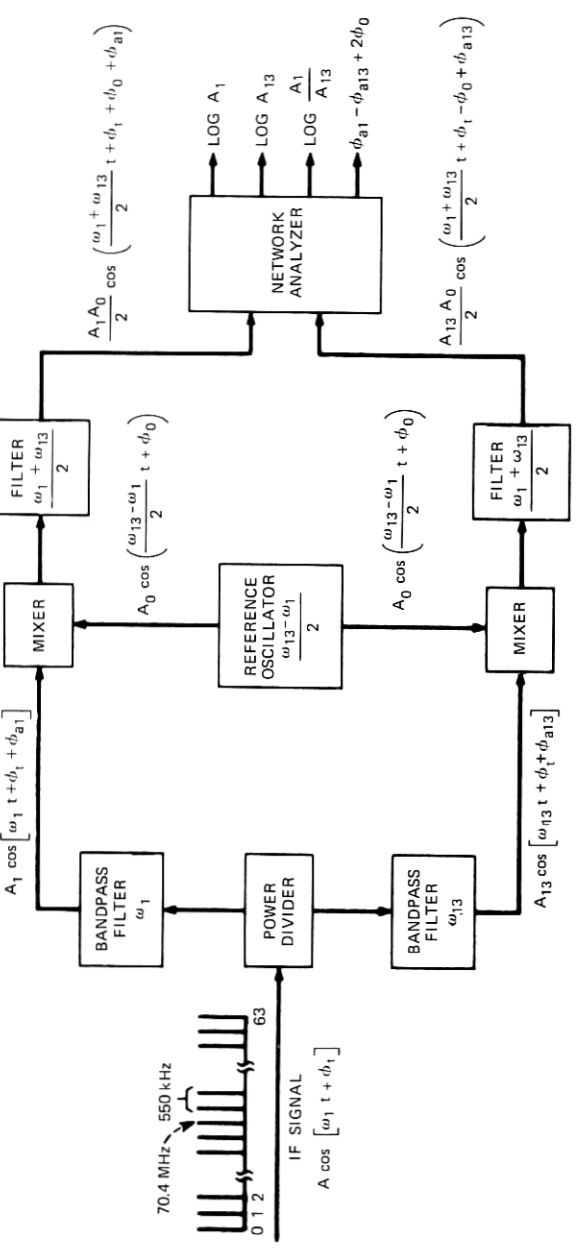

Fig. 1—Basic schematic of two-channel phase and amplitude comparator.

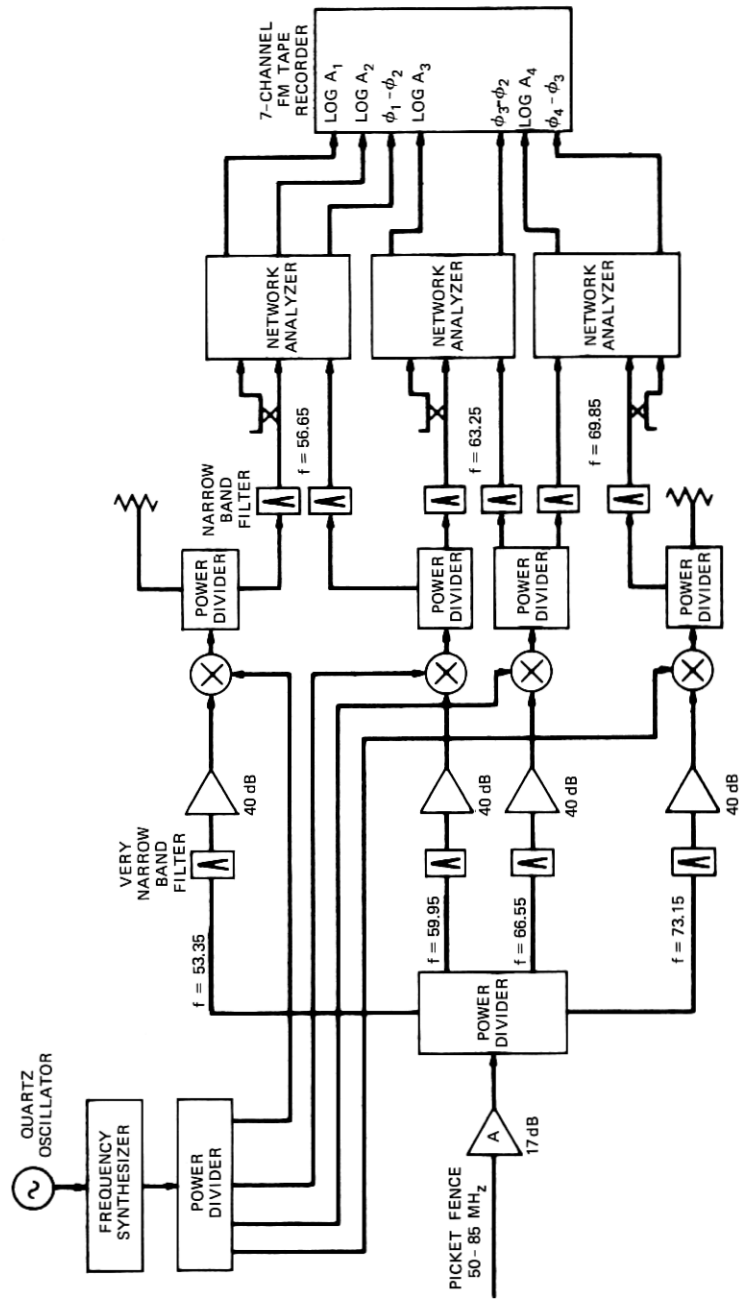

Fig. 2—Schematic of the system.

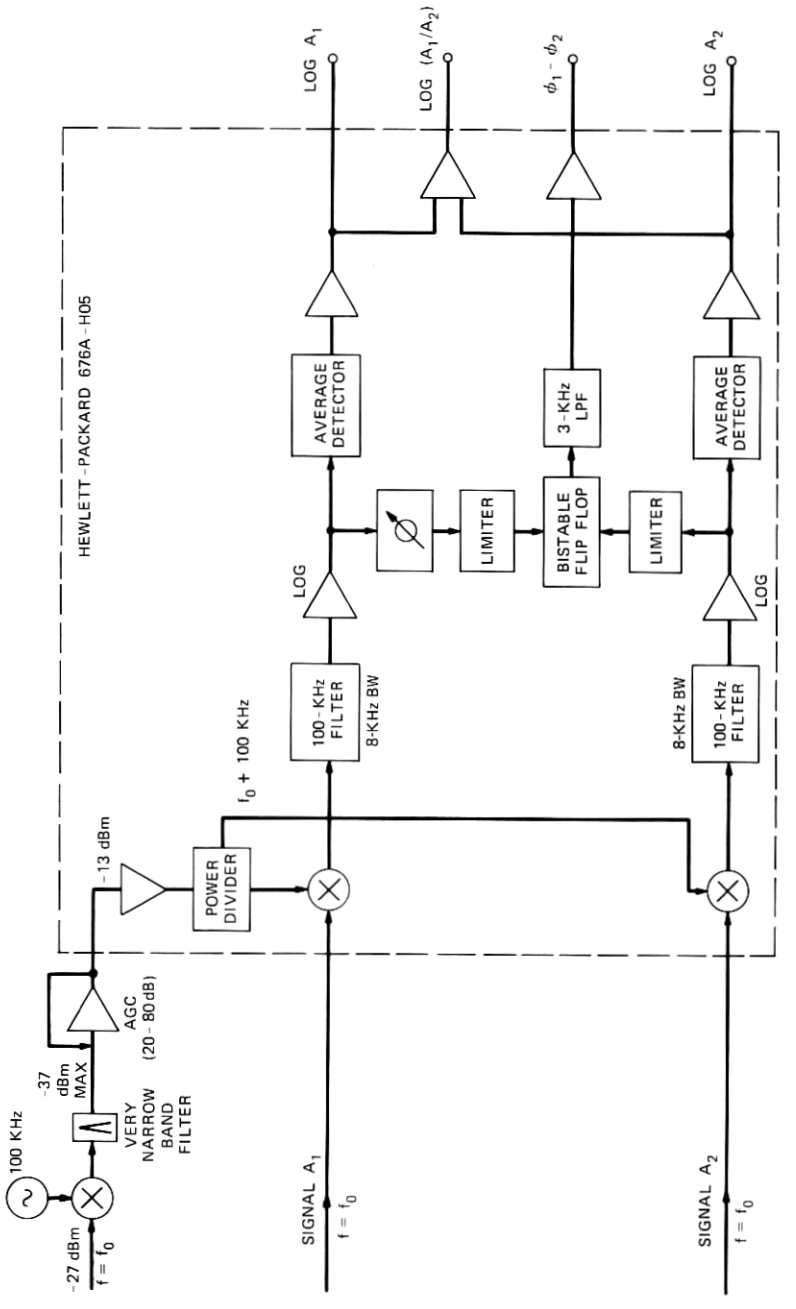

Fig. 3—Network analyzer.

amplitudes and three phase differences are recorded. Note that if one knows $\Phi_2 - \Phi_1$ and $\Phi_3 - \Phi_2$ one can compute $\Phi_3 - \Phi_1$, etc.

III. DISCUSSION OF EXPERIMENTAL TECHNIQUE

The experimental technique described here has several advantages and limitations compared with others used in the past.[3-5]

The distinguishing characteristic of this technique is that the actual phase difference between two signals is measured. Thus, if we consider $\Phi = \Phi(\omega)$, we measure $\Delta\Phi/\Delta\omega$ rather than simply $d^2\Phi/d\omega^2$, which is the delay distortion. Further, the tones are generated and measured at IF in such a way that the phase and frequency variations of the up and down converters do not affect the measurements. Hence, the same apparatus could be used at any desired carrier frequency. A knowledge of the envelope delay, $d\phi/d\omega$, could be of use in the analysis of multipath fading of line-of-sight microwave link.

The basic problem facing anyone wishing to measure phase differences of the same signal reaching two widely separated receivers, as in very-long-baseline interferometry (VLBI) or, as in our case, of two signals generated at one place and received at another, is one of a time reference. One technique is to transmit a timing signal either over the air or through a cable from one place to another. This approach suffers from unknown variations in the signal path because of atmospheric changes in the broadcast case or temperature variations in the cable case. Following the lead of the workers in VLBI, similar standard oscillators have been set up at the transmitter and receiver. These oscillators have sufficient short-term (<1 s) and long-term (<1 degree/day) stability to enable measurements to be made within the desired accuracy (0.03 degree rms for 6.6-MHz tone separation).

IV. CHARACTERISTICS OF FADES

This section describes the temporal behavior of the signal during fading. The data were recorded on analog FM tapes continuously from September 11 to December 31, 1970. The system was shut down on two occasions for several days for servicing. The system was also turned down a few times for several hours at a time for making tests. The tape was manually changed as it approached the end. Each tape lasted an average of five days. The tape was turned on automatically whenever any one tone exceeded 10-dB fade and ran till all the four tones recovered from deeper than 10-dB fade. The nature of the fades can be classified into the following broad categories.

(*i*) All the four tones in the 20-MHz band fade simultaneously, with the level of fade being approximately the same for all of them. In other words, there is no significant frequency selectivity present. Such fades last several minutes. These fades are usually relatively shallow (less than or about 20 dB).

(*ii*) The four tones fade selectively; that is, the fade levels of the four tones are significantly different. Such selective fades are usually deep (greater than about 20 dB) and last no more than a few seconds and often much less than one second. The dispersive fades are usually superimposed on shallow, nondispersive ones. The deepest fade level on the four tones may occur either simultaneously or separated in time by a small fraction of a second. In the former case the minimum amplitude in the band occurs at a single frequency in the band, whereas in the latter case the minimum traverses across the band in time.

There is no significant phase nonlinearity during the nondispersive fades mentioned in case (*i*) above. A temporal presentation of the amplitudes of the four tones and phase differences between them during a typical nondispersive fade is given in Fig. 4. For the sake of clarity, the traces are displaced from one another. The fade level of A_1 is with respect to its nominal unfaded value. The nominal unfaded levels of A_2, A_3, and A_4 are displaced by approximately 20, 40, and 60 dB, respectively. Similarly, the three phase difference traces are displaced from each other by about 50 degrees. The fade duration is about 1 minute, and the maximum fade depth is about 15 dB. There is no noticeable variation in the magnitudes of the difference between adjacent tones. Although the traces of the phase differences in Fig. 4 are nearly horizontal, they have, in general, a linear slope with time which is the same for all three. As mentioned in Section II, this is caused by the difference in the quartz oscillator frequencies between the one driving the picket-fence generator at the transmitter and that of the other in the phase/amplitude measuring system at the receiver. Any path length change is reflected on the three traces as a change from the linear slope and will be the same in all the three traces. However, when there is a phase nonlinearity present within the 20-MHz band, the three traces will have different slopes.

Figure 5 represents a dispersive fade of the type discussed in case (*ii*) above. The total duration of the fade is in excess of 5 minutes, and the maximum fade depth is 39 dB (on A_4). Once again, the time axis has been referenced with respect to that at which the deepest

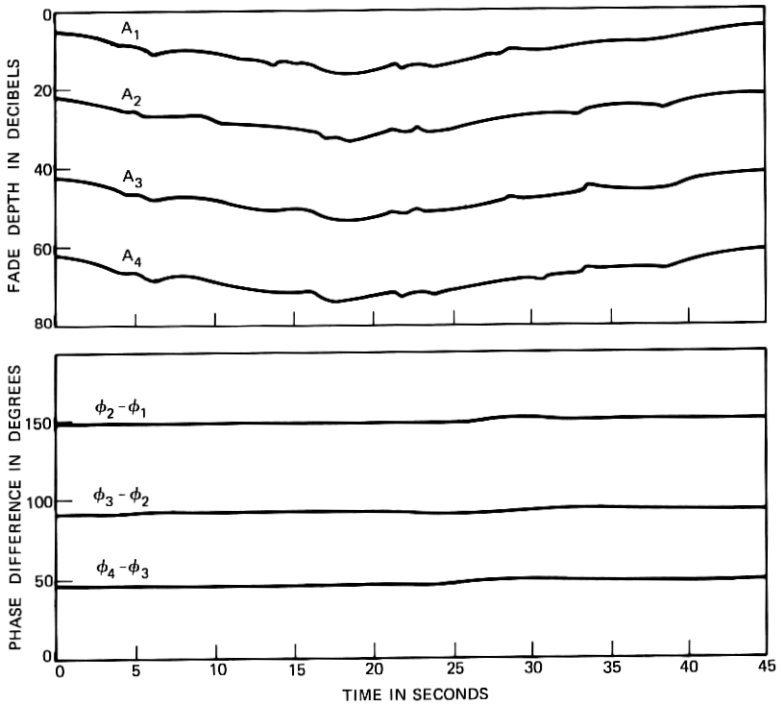

Fig. 4—Nondispersive fading.

fade occurs. It could be observed in this particular event that there are two deep fades separated by about 2 minutes superimposed on the prolonged shallow fades. It is further observed from the phase data that significant phase nonlinearity is present only during the deep fade periods that last only in the order of seconds. The magnitude of the phase nonlinearity is dependent on the depth of the fade and its amplitude dispersion. Thus, while the first fade in Fig. 5 exhibits significant phase nonlinearity, the second does not.

A time-expanded representation of the first fade in Fig. 5 is given in Fig. 6. Large selective fading is exhibited during this event for an extended period of time. During the few seconds around the deepest fade period, the fade dispersion curve changes slope and the high-frequency end of the band (A_4) fades deeper than the rest. The phase nonlinearity is exhibited predominantly during this period of deepest fade. Figure 6 has been redrawn in Fig. 7 by interchanging the role of time and frequency parameters. The dispersion with respect to fre-

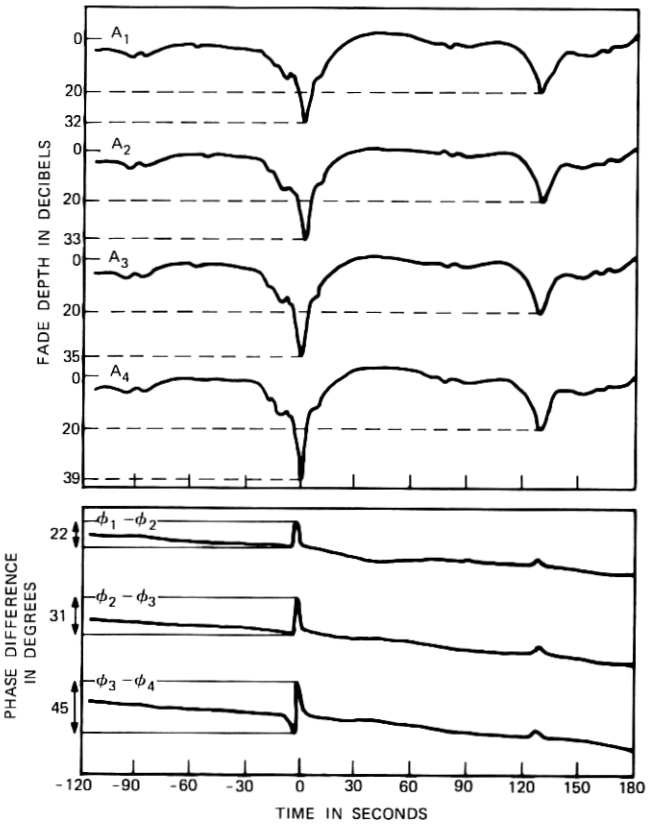

Fig. 5—Dispersive fading.

quency of the fade depth and the phase difference are plotted as discrete functions of time. This presentation visually portrays the nonlinearities as greatest around zero time. We can also observe that the phase difference curve changes from a convex to a concave shape between 0 and 0.2 second. Thus, the phase nonlinearity could assume zero value around the time of deepest fade.

The relationship between the amplitude distortion and phase nonlinearity was explored by fitting a second-order polynomial curve over the log-amplitude and phase dispersion curves and then correlating the coefficients of the quadratic terms.

The following second-order polynomial expansion was assumed for log-amplitude dispersion $\chi(f)$ (in dB) and phase dispersion $\phi(f)$ (in

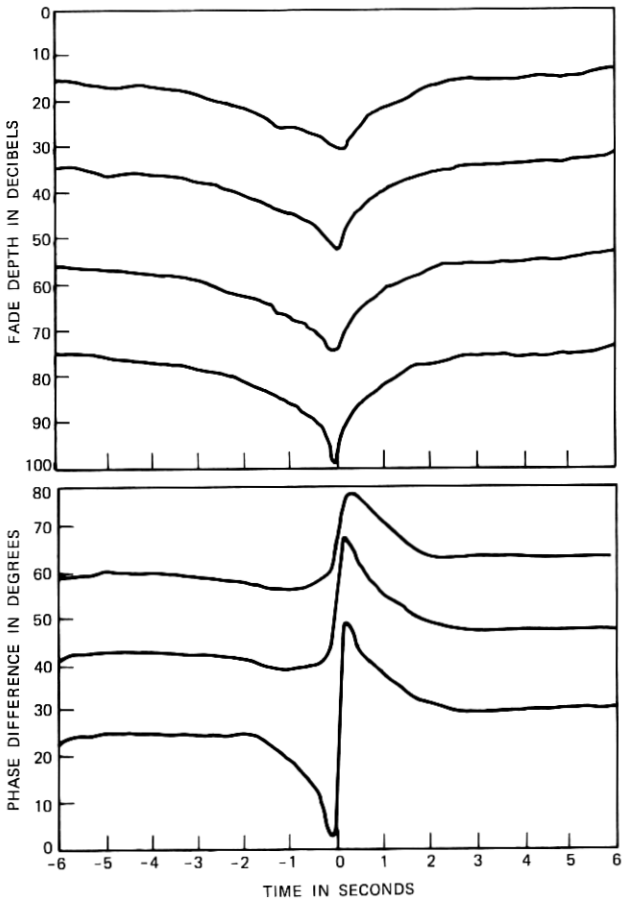

Fig. 6—Dispersive fading.

degrees).

$$\chi(f) = a_\chi(f_3) + b_\chi(f - f_3) + c_\chi(f - f_3)^2 \tag{11}$$

$$\phi(f) = a_\phi(f_3) + b_\phi(f - f_3) + c_\phi(f - f_3)^2. \tag{12}$$

The temporal behavior of the quadratic log-amplitude and phase nonlinear coefficients designated by c_χ and c_ϕ, respectively, are given in Fig. 8. There appears to be some degree of correlation between these coefficients except around zero time reference. As explained in the description of Fig. 7, the reason for the deviation around zero time is the change in the convexity of the phase dispersion curve.

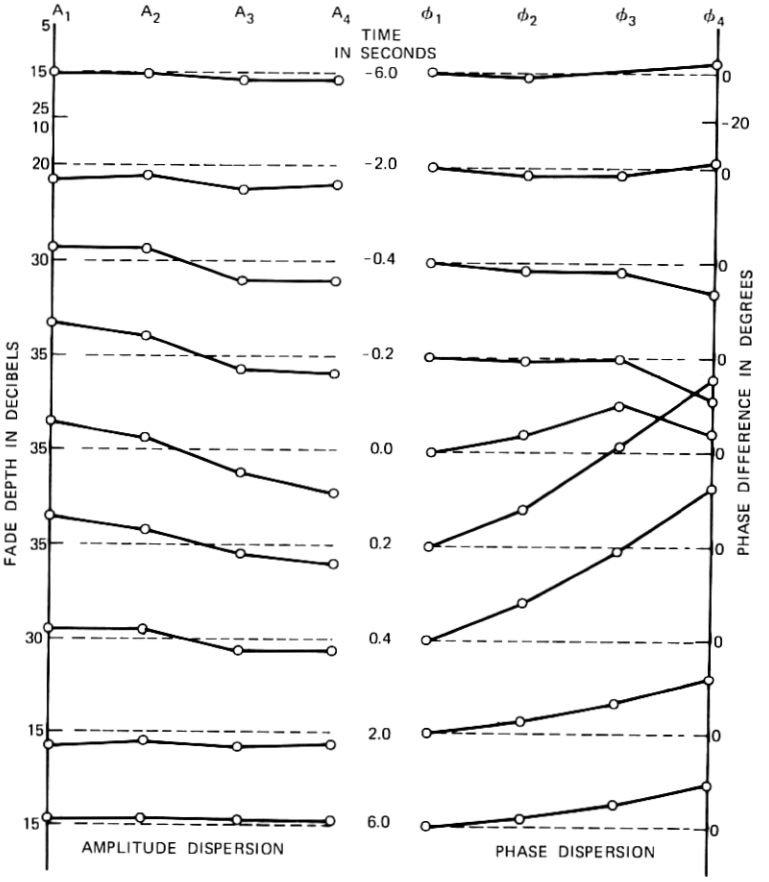

Fig. 7—Amplitude and phase dispersion during dispersive fade.

V. DATA ANALYSIS

The amplitude and phase dispersion data have been fitted with second-order polynomial curves, and the nonlinear coefficients of the two have been studied. Specifically, results on the following have been obtained.

(*i*) The distribution curve describing the fraction of time that the phase nonlinearity exceeds a given value.
(*ii*) The average of the magnitude of the phase nonlinearity as a function of the depth of the fade.

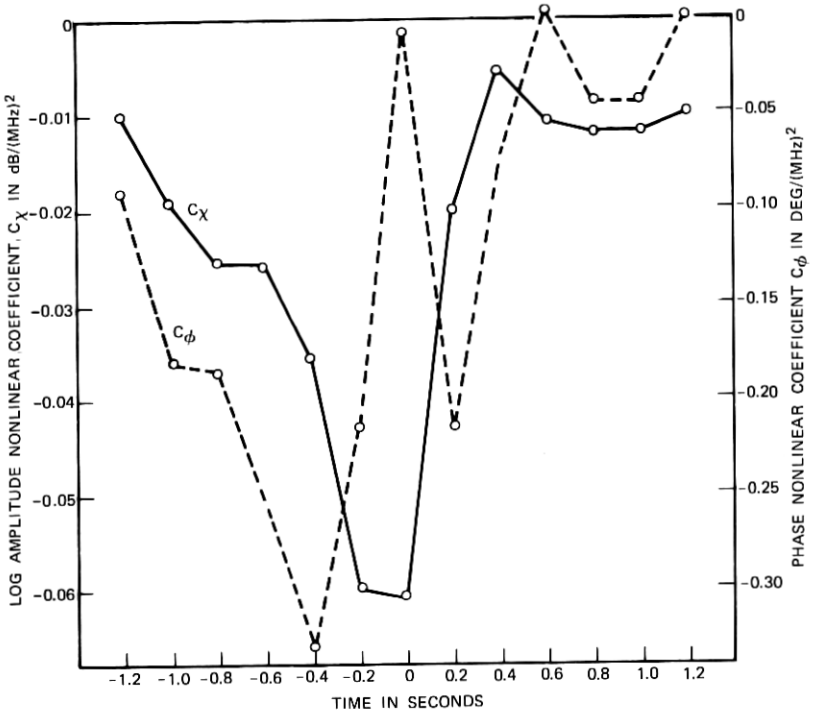

Fig. 8—Temporal behavior of log-amplitude and phase nonlinearities (c_χ, c_ϕ).

(*iii*) The nature of the correlation between log-amplitude and phase nonlinear coefficients.

Letting $f_3 = 0$ and $f - f_3 = \Delta f$ in eqs. (11) and (12), we obtain

$$\chi(\Delta f) = a_\chi(0) + b_\chi(\Delta f) + c_\chi(\Delta f)^2 \tag{13}$$

$$\phi(\Delta f) = a_\phi(0) + b_\phi(\Delta f) + c_\phi(\Delta f)^2. \tag{14}$$

The data were taken on four tones, at $\Delta f = -13.2$ MHz, -6.6 MHz, 0, and $+6.6$ MHz. For the sake of convenience in the analysis, the frequency separation was normalized with respect to $\Delta f = 13.2$ MHz. Thus, the four data points corresponding to eq. (14) were designated by the following set of simultaneous equations.

$$\begin{aligned}
\phi(-1) &= \tilde{a}_\phi(0) + \tilde{b}_\phi(-1) + \tilde{c}_\phi(-1)^2 \\
\phi(-\tfrac{1}{2}) &= \tilde{a}_\phi(0) + \tilde{b}_\phi(-\tfrac{1}{2}) + \tilde{c}_\phi(-\tfrac{1}{2})^2 \\
\phi(0) &= \tilde{a}_\phi(0) \\
\phi(+\tfrac{1}{2}) &= \tilde{a}_\phi(0) + \tilde{b}_\phi(\tfrac{1}{2}) + \tilde{c}_\phi(+\tfrac{1}{2})^2.
\end{aligned} \tag{15}$$

Comparing the coefficients of eqs. (14) and (15), we obtain

$$\begin{aligned} a_\phi &= \tilde{a}_\phi \\ b_\phi &= \tilde{b}_\phi \left(\frac{1}{2 \times 6.6 \times 10^6} \right) \\ c_\phi &= \tilde{c}_\phi \left(\frac{1}{2 \times 6.6 \times 10^6} \right)^2 . \end{aligned} \tag{16}$$

A similar set of equations can be obtained for the log-amplitude dispersion, yielding

$$\begin{aligned} a_\chi &= \tilde{a}_\chi \\ b_\chi &= \tilde{b}_\chi \left(\frac{1}{2 \times 6.6 \times 10^6} \right) \\ c_\chi &= \tilde{c}_\chi \left(\frac{1}{2 \times 6.6 \times 10^6} \right)^2 . \end{aligned} \tag{17}$$

The measured log-amplitude and phase dispersion data of each event was digitized at a sampling period of 0.2 second. Equations (15) contain three unknowns ($\tilde{a}_\phi$, $\tilde{b}_\phi$, and $\tilde{c}_\phi$) and four equations. The four data points for ϕ were obtained by arbitrarily setting $\phi_1 = 0$ and then computing ϕ_2, ϕ_3, and ϕ_4 by the measured differences. These four data points were then fitted with a smooth curve with the least-square-fit criterion, and c_ϕ was computed for the fitted curve. Note that this procedure does not affect the computational result on c_ϕ. Further, it will not cause any serious error as discussed by Babler,[1] as in the case of fitting a third-order polynomial curve that passes through all four data points. The log-amplitude coefficient c_χ was obtained by fitting a second-order polynomial curve through the four data points, χ_1, χ_2, χ_3, and χ_4, which are directly available from measurements. The coefficients c_ϕ and c_χ were then computed using eqs. (16) and (17).

The quadratic phase nonlinearity can easily be related to the more familiar parameter of delay distortion. The delay distortion, denoted by $\tau(\omega)$, is defined as the departure of the envelope delay, $D(\omega)$, from a constant value.[6] The envelope delay is given by[6]

$$D(\omega) = \frac{d\phi}{d\omega} . \tag{18}$$

From eqs. (12) and (18), we obtain

$$\tau(\Delta\omega) = \frac{c_\phi}{180 \times 10^{+6}} (\Delta f), \tag{19}$$

where $\tau(\Delta\omega)$ is the delay distortion in s/MHz, c_ϕ is expressed in degrees/(MHz)^2, and Δf is expressed in MHz.

VI. RESULTS

Numerous fading events were recorded exceeding 10-dB fade. Of these, 26 events faded deeper than 20 dB and were selected for data analyses. This selection was based on the fact that only these display phase distortion and consequently are of interest here. The first selected event occurred during the period of September 16 to 18 (recorded in the tape that ran during this period). The twenty-sixth event occurred during the period of November 20 to 23. No event exceeded 20-dB fade between November 23 and December 31. Babler[1] has observed, in the amplitude dispersion experiment run during approximately the same period in the same microwave link, 40 counts of the tone at the center of the band dipping below 20 dB. In the present analysis, the interval of an event is defined beginning from when at least one tone exceeds a fade depth of 10 dB and lasting until all the tones have recovered above 10-dB fade level. Thus, an event of ours could include more than one count of Babler's experiment. Considering the loss of time because of system shut-downs and tape run-outs mentioned in the previous section, the number of 20-dB fade events in the two experiments agree with each other satisfactorily. Note that the number of fading events during the 1970 autumn season appears to be significantly below normal. Unfortunately, not all the events could be used in the analyses because of failure in part of the instrumentation. Data of 16 events were used in connection with the analysis of phase nonlinearity [items (*i*) and (*ii*) mentioned in the previous section], and the correlation between log-amplitude and phase nonlinearities [item (*iii*)] was made for 14 events.

6.1 *Distribution of Phase Nonlinearity*

The distribution of the phase nonlinear coefficient c_ϕ for the pooled data of 16 events (consisting of 2284 samples) is shown in Fig. 9. Three distribution curves represent the positive, the negative, and the absolute values of c_ϕ. Observe in Fig. 9 that 70 percent of the samples yielded positive values for c_ϕ and the remaining 30 percent were negative. No attempt was made to study the distributions of the individual events, since the sample size was considered inadequate. The distribution of $|c_\phi|$ is presented on a log-normal graph in Fig. 10. Observe that the smooth curve fitted over the data points is "close"

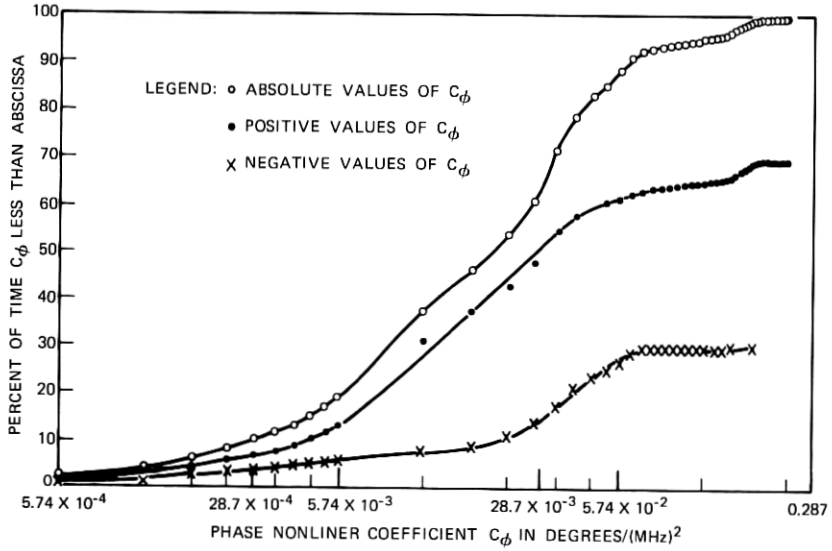

Fig. 9—Distribution curves for c_ϕ.

to a straight line. Hence, it appears that the distribution of the phase nonlinearity is close to log-normal. This conclusion is substantiated more quantitatively in the appendix.

6.2 *Dependence of Phase Nonlinearity on Fade Depth*

Figure 11 shows the dependence of phase nonlinearity on the depth of fade. The data points represent the magnitude of quadratic nonlinear coefficient $|c_\phi|$ as each event reached the fade depths of 10, 15, 20, 25, 30, 35, and 40 dB as well as when they come out of the fade. This approach of plotting the data points was adopted over that of recording the value of $|c_\phi|$ at the maximum level of the fade for each event for the following two reasons. First, the sample size is larger. Second, and more important, as explained in Section IV, $|c_\phi|$ could momentarily assume a zero value at the peak of the fade because of its changing sign, and thus could lead to an erroneous result. The smooth curve represents the average value of $|c_\phi|$ as a function of the fade depth. We see that $|c_\phi|$ increases with fade depth beyond 20-dB fade. The magnitude of $|c_\phi|$ remains constant at 0.02 degree/(MHz)^2 below 20 dB, which is due to the limitation in the accuracy of equipment and the variance of $|c_\phi|$ in curve fitting. ($|c_\phi|$ should eventually go to zero at 0-dB fade.)

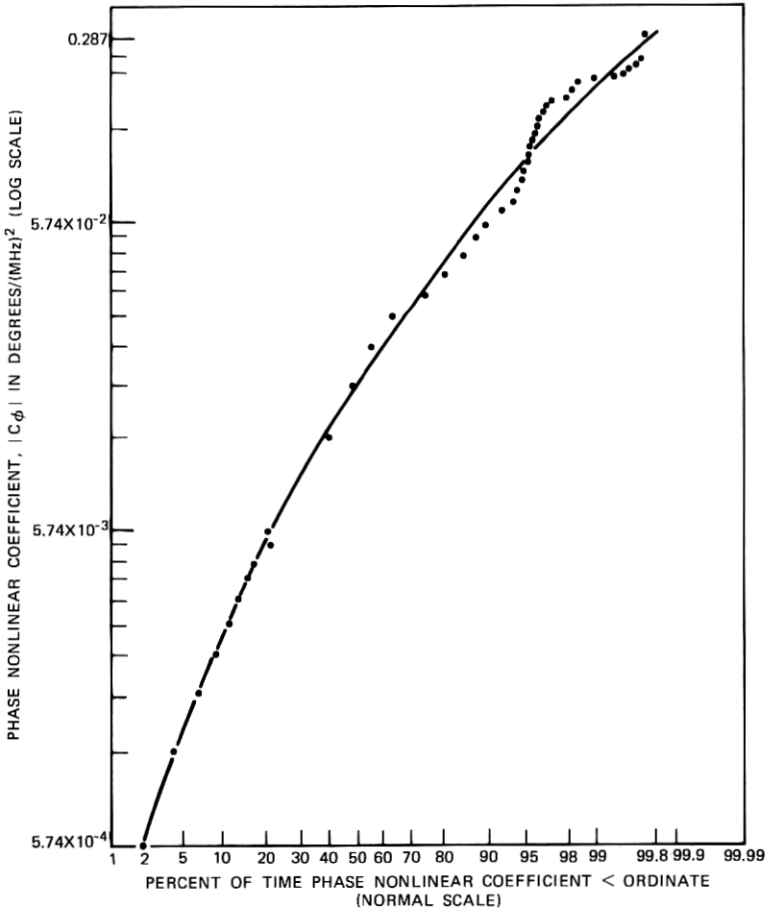

Fig. 10—Distribution curve for $|c_\phi|$: log-normal plot.

Also presented in the ordinate scale is the delay distortion $\tau(\Delta\omega)$ in eq. (19), in seconds over a 1-MHz band. Observe that corresponding to $|c_\phi| = 0.1$ degree/(MHz)^2 and $\Delta\omega = 2\pi$ the delay distortion is calculated to be 0.55 nanosecond, and this occurs at a fade depth of about 34 dB. This reasoning does not take into account the phase dispersion ripples being present between the tones (i.e., frequency separation of less than 6.6 MHz). Babler[1] and Ho[7] have reported the presence of such ripples (some of them of significant magnitude) superposed on an overall smooth amplitude dispersion curve in a 20-MHz band. This fine structure is currently being investigated in a

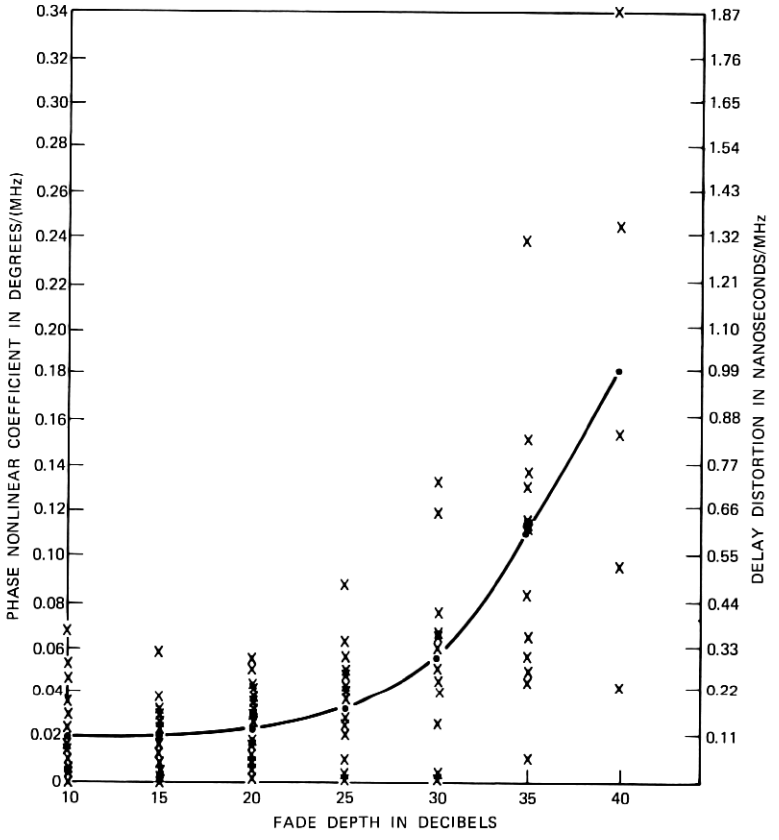

Fig. 11—Dependence of phase nonlinearity, c_ϕ, on fade depth.

more comprehensive study being conducted at Bell Laboratories by choosing tones that are closer than 6.6-MHz separation.

6.3 *Correlation Between Log-Amplitude and Phase Nonlinearities*

The correlation between the log-amplitude nonlinearity $\tilde{c}_\chi$ and phase nonlinearity $\tilde{c}_\phi$ was computed for each event. Table I shows the results for 14 events. The correlation coefficient was calculated for each event using digitized data points for that part of the fade below the 10-, 15-, 20-, and 25-dB levels in order to establish the dependence of the correlation coefficient R on fade level. The results shown in Table I do not easily lend themselves toward making any firm conclusions about the physical model that would yield such data, yet they are presented here

TABLE I—CORRELATION BETWEEN LOG-AMPLITUDE AND PHASE NONLINEARITIES

Event	$R(\tilde{c}_x; \tilde{c}_\phi)$			
	10 dB	15 dB	20 dB	25 dB
70-3-1	+0.58	+0.58	+0.68	+0.77
70-3-2	−0.38	−0.40	−0.71	—
70-6-1	+0.80	+0.80	+0.60	+0.36
70-6-2	+0.68	+0.68	+0.70	+0.70
70-6-4	+0.50	+0.43	—	—
70-6-5	+0.49	+0.49	−0.70	—
70-6-6	+0.36	+0.39	+0.45	−0.48
70-6-8	+0.68	+0.93	—	—
70-13-1	−0.74	−0.74	—	—
70-16-1	−0.65	−0.67	−0.70	−0.71
70-16-2B	−0.39	−0.62	−0.74	—
70-18-1A	−0.65	−0.64	−0.71	−0.72
70-18-1B	−0.97	−0.97	−0.98	−0.99
70-23-1	−0.42	−0.42	−0.48	−0.48

to give an idea of the complexity of the problem. The following observations can be made on the results.

(*i*) The positive and negative coefficients are equally probable.

(*ii*) The magnitude of the correlation coefficient, in general, increases as the fade-depth increases.

(*iii*) The correlation coefficient, in some cases, changes sign near the peak of the fading.

(*iv*) It appears difficult to predict the behavior of the phase nonlinear coefficient from a knowledge of the amplitude nonlinear coefficient. One primary aim in pursuing this course of analysis was to investigate whether a deterministic relationship could be established between the two coefficients. If this were possible, it would have helped a communication system designer to build an automatic phase compensator that could be controlled by measuring the amplitude dispersion, measurement of the amplitude dispersion being far simpler than that of the phase dispersion.

VII. SUMMARY

Measurement of phase and amplitude dispersion have been made over a 20-MHz band at 6 GHz on a 42-km line-of-sight radio link. The present experimental technique is unique in that the direct phase dispersion, instead of delay distortion, has been measured using the

scheme of very-long-base interferometry. The base delay between adjacent pairs of four tones equally spaced over a 19.8-MHz band was measured. Twenty-six events were recorded during the autumn season of 1970 that produced phase distortion of greater than 0.02 degree/(MHz)^2. All these events had fades which exceeded 20 dB below the nominal level. Although the number of events observed appears to be considerably less than normal, it was considered adequate to derive some preliminary statistics about the phase dispersion characteristics during deep dispersive microwave fading.

The quadratic phase nonlinear coefficient which is linearly proportional to the delay distortion is observed to have a log-normal distribution. To the best of the authors' knowledge, this is the first time that statistics have been obtained on such phase characteristics. These results may be useful in the formulation of a statistical model of microwave fading.

The quadratic phase nonlinear coefficient and hence the delay distortion increase with the depth of fade. On the average, fades deeper than 34 dB below nominal level cause a delay distortion in excess of 0.55 nanosecond/MHz. For a monochrome television signal with about 4-MHz bandwidth, the delay distortion permitted is about 25 nanoseconds.[6] If the same bandwidth is assumed at the radio frequency band as would be if it were an amplitude-modulated system, the average delay distortion for a 40-dB fade would be, from Fig. 11, about 4 nanoseconds, which would be well within the tolerance. Over the measured 20-MHz band, the delay distortion at 40-dB fade would be about 20 nanoseconds.

During the deep dispersive fades, the nonlinear phase and amplitude coefficients were found to have nonzero correlation which could be either positive or negative. No simple relationship seems apparent between the two coefficients. Although simple two-ray models can be made to account for both amplitude and phase dispersion,[7] the complex temporal behavior indicated in our results along with that reported by Babler[1] lead us to believe that the multiray (more than two rays) phenomenon is the cause of these deep fades.

VIII. ACKNOWLEDGMENTS

The authors wish to recognize the assistance of D. E. Kreichbaum in the data reduction and A. M. Franz in the data processing. W. T. Barnett's comments concerning the improved presentation of the results is gratefully acknowledged.

APPENDIX

To determine the nature of the distribution curve for the absolute value of c_ϕ, an entirely empirical approach to the problem was adopted. Plotting the raw data of the phase nonlinear coefficient $|\tilde{c}_\phi|$ on a log-normal graph paper indicated that the distribution was close to log-normal. In the literature[8] a powerful technique exists which transforms, in most cases, a given distribution to a normal distribution by a suitable linear transformation. Use of this technique was expected to yield information on how closely the observed set of data approximated a log-normal distribution. Following Box and Cox[8] who have treated such an analysis of transformation, the following transformation was chosen.

$$\tilde{c}_{\phi t}(\lambda) = \begin{cases} \dfrac{\tilde{c}_\phi^{\lambda} - 1}{\lambda} & (\lambda \neq 0) \\ \log \tilde{c}_\phi & (\lambda = 0). \end{cases} \tag{20}$$

Here, λ is the parameter that defines the transformation. (For the sake of convenience, the absolute value signs have been omitted.) In accordance with our assumption, a value exists for λ such that $\tilde{c}_{\phi t}(\lambda)$ is normally distributed. The value of λ can be determined using the maximum likelihood theory. The method of maximum likelihood involves maximizing the log-likelihood estimate $\mathfrak{L}_{\max}$ with respect to the unknown parameters of μ, σ^2, and λ, where μ and σ^2 are the mean and variance of the transformed data $\tilde{c}_{\phi t}(\hat{\lambda})$. The maximum likelihood estimate of λ, denoted by $\hat{\lambda}$, yields the best possible estimate that would make the transformed variable $\tilde{c}_{\phi t}$ closest to a normal distribution. The maximum log-likelihood function is given by

$$\mathfrak{L}_{\max}(\lambda/\tilde{c}_{1\phi}, \tilde{c}_{2\phi}, \cdots, \tilde{c}_{n\phi}) = -\frac{n}{2}\log \sigma^2 + (\lambda - 1)\sum_{i=1}^{n} \log \tilde{c}_{i\phi}, \tag{21}$$

where n is the number of data points.

The value of λ varied between -1 and $+1$ in steps of 0.1. The maximum value of $\mathfrak{L}_{\max}(\lambda)$ as a function of λ occurs at $\lambda = -0.1$. Thus, the maximum likelihood estimate for λ, $\hat{\lambda}$ is -0.1. Figure 12 shows the data points of $\tilde{C}_{\phi t}(\hat{\lambda})$ on a log-normal graph. The straight line through the data points corresponds to $\lambda = 0$. It is seen from eq. (20) that $\lambda = 0$ yields a log-normal distribution. Except at the large value of nonlinearity, the distribution appears log-normal. This is further justified by the fact that $\hat{\lambda} = -0.1$ is statistically quite

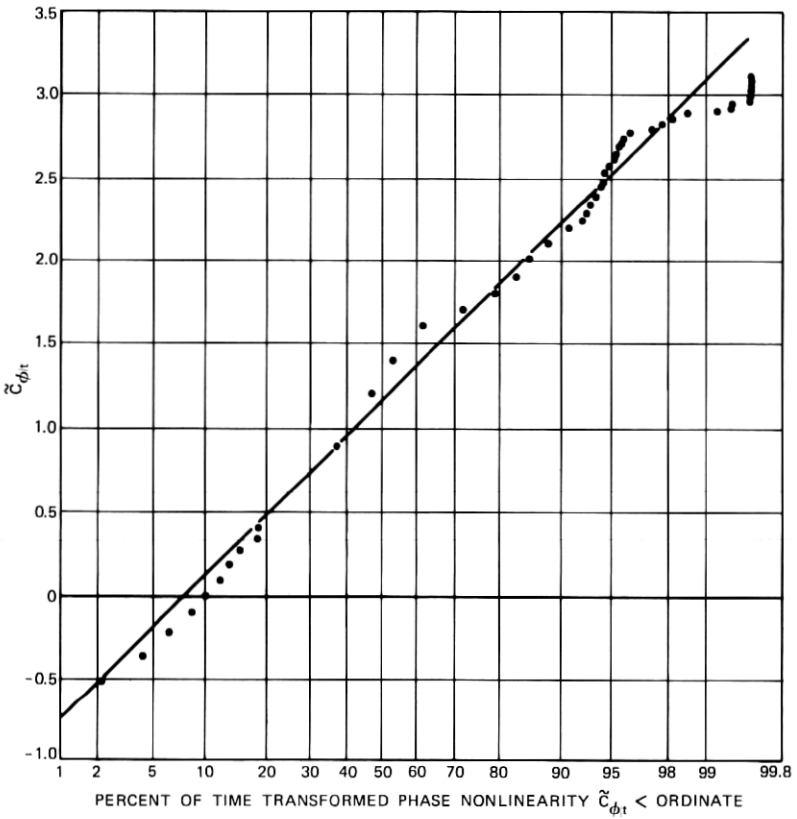

Fig. 12—Distribution of $\tilde{c}_{\phi t}(\hat{x})$: log-normal plot: $\hat{\lambda} = -0.1$.

close to zero. The deviation at the high end can be largely attributed to poor sample size.

REFERENCES

1. Babler, G. M., "A Study of Frequency Selective Fading for a Microwave Line-of-Sight Narrowband Radio Channel," B.S.T.J., *51*, No. 3 (March 1972), pp. 731–757.
2. Kaylor, R. L., "A Statistical Study of Selective Fading of Super-High Frequency Radio Signals," B.S.T.J., *32*, No. 5 (September 1953), pp. 1187–1202.
3. Thompson, M. C., Jr., and Vetter, M. J., "Single Path Phase Measuring System for Three Centimeter Radio Waves," Rev. Sci. Instr., *29*, No. 2 (February 1958), pp. 148–150.
4. Thompson, M. C., Jr., and Janes, H. B., "Measurements of Phase Stability Over a Low-Level Tropospheric Path," J. Res. NBS, *63P*, July-August 1959, pp. 45–51.

5. Janes, H. B., "Correlation of the Phase of Microwave Signals on the Same Line-of-Sight Path at Different Frequencies," IEEE Trans. Ant. Prop., November 1963, pp. 716–717.
6. Bell Telephone Laboratories, Incorporated, *Transmission Systems for Communication Engineers*, Fourth Edition (February 1970), p. 721.
7. Ho, T. L., private communication.
8. Box, A. E. P., and Cox, D. R., "An Analysis Transformation," Royal Statistical Society, Series B, *26*, No. 2 (1964), pp. 211–252.